EUKARYOTIC CELL, Aug. 2009, p. 1146–1154 Vol. 8, No. 8
1535-9778/09/$08.00+0 doi:10.1128/EC.00061-09

Characterization of Two Putative Protein Translocation Components in the Apicoplast of *Plasmodium falciparum*▽†

Ming Kalanon, Christopher J. Tonkin,‡ and Geoffrey I. McFadden*

School of Botany, University of Melbourne, Parkville, Victoria, Australia, 3010

Received 23 February 2009/Accepted 1 June 2009

Protein trafficking to the stroma of the apicoplast of *Plasmodium falciparum* requires translocation across several membranes. To further elucidate the mechanisms responsible, we investigated two proteins: *P. falciparum* Tic22 (PfTic22), a putative component of the translocon of the inner chloroplast membrane; and PfsDer1-1, one of two homologues of the *P. falciparum* symbiont-derived Der1 (sDer1) protein, a putative component of an endoplasmic reticulum-associated degradation (ERAD) complex in the periplastid membrane. We constructed parasites expressing hemagglutinin (HA)-tagged PfTic22 and PfsDer1-1 under the control of their endogenous promoters using the 3′ replacement strategy. We show that both PfTic22-HA and PfsDer1-1-HA are expressed predominantly during the trophozoite stage of the asexual replication cycle, which corresponds to the most dynamic stages of apicoplast activity. Although both proteins localize to the periphery of the apicoplast, PfTic22-HA is a membrane-associated protein while PfsDer1-1-HA is an integral membrane protein. Phylogenetic analysis indicates that PfsDer1-1 is one of two Der1 paralogues predicted to localize to the apicoplast in *P. falciparum* and that it has orthologues in diatom algae, supporting the chromalveolate hypothesis. These observations are consistent with putative roles for PfTic22 and PfsDer1-1 in protein translocation into the apicoplast of *P. falciparum*.

Plasmodium falciparum, the causative agent of malaria, contains a plastid known as the apicoplast that is essential for parasite survival in its erythrocytic (7) and liver life stages (35, 40). Although the apicoplast is not photosynthetic, it houses several plastid-like biochemical pathways including the biosynthesis of fatty acids, isoprenoids, heme, and iron-sulfur clusters (23). Apicoplasts also have prokaryote-derived mechanisms for replication of their DNA, transcription, and translation (3, 25). Like other plastids, apicoplasts originate from a bacterial endosymbiont, and this makes them a promising target for novel therapeutics for the treatment of malaria, one of the world's most serious diseases (24).

Generally, apicoplasts occur in members of the phylum *Apicomplexa*, which includes several parasites of humans such as *P. falciparum*, the causative agent of the most lethal form of malaria, and *Toxoplasma gondii*, which causes toxoplasmosis. Other apicomplexan parasites, such as *Theileria* and *Babesia*, cause disease in livestock and severely impact agricultural practice. The only apicomplexan genus known to lack an apicoplast is *Cryptosporidium*, which is believed to have lost the organelle (41). The recent discovery of a photosynthetic apicomplexan, the coral symbiont *Chromera velia* (19), strongly supports the hypothesis that apicoplasts were originally photosynthetic and ultimately derived from a phagotroph engulfing a free-living red alga, a process known as secondary endosymbiosis (2, 8).

The apicoplast of *P. falciparum* contains a small, highly condensed circular genome of 35 kb that encodes about 52 genes (38). The apicoplast genome is clearly a remnant plastid genome that has undergone loss of all photosynthesis genes plus extensive transfer of genes from the endosymbiont to the host nucleus during endosymbiosis (17). As a consequence, the majority of the apicoplast's protein complement must be transported back to the organelle posttranslationally, a process complicated by the fact that the organelle is surrounded by four membranes. The localization signals required for trafficking most proteins back to the apicoplast of *P. falciparum* have been well established and comprise an N-terminal leader consisting of a hydrophobic signal peptide and a plastid-targeting transit peptide enriched in basic amino acids and asparagines (6). Together, this bipartite leader is sufficient and necessary to target proteins to the stroma of the apicoplast via the endomembrane secretory system (30, 37).

Transit peptides of the *P. falciparum* apicoplast are similar to plant chloroplast transit peptides in that they vary significantly in length and contain no consensus sequences or conserved secondary structures (22). However, we have previously shown that the presence of basic residues, regardless of their positions within the transit peptide, in addition to the depletion of acidic residues, is important for apicoplast targeting (28). Furthermore, Hsp70 binding is likely to be involved since disruption of Hsp70 binding sites within an apicoplast transit peptide markedly reduces transit peptide fidelity (6, 28). Indeed, there seems to be little else that defines a transit peptide because completely artificial sequences can mediate targeting from the endomembrane system into the apicoplast (28). This degenerate amino acid bias within the transit peptide allowed the development of two robust apicoplast-targeted protein pre-

* Corresponding author. Mailing address: School of Botany, University of Melbourne, Parkville, Victoria, Australia 3010. Phone: 61 3 8344 5053. Fax: 61 3 9347 5460. E-mail: gim@unimelb.edu.au.

‡ Present address: Division of Infection and Immunity, The Walter and Eliza Hall Institute of Medical Research, Parkville, Victoria, Australia 3050.

† Supplemental material for this article may be found at http://ec.asm.org/.

▽ Published ahead of print on 5 June 2009.

diction algorithms, PATS (42) and PlasmoAP (6). These algorithms have been used to predict the proteome of the apicoplast of *P. falciparum*, estimated at almost 500 proteins (23).

While the role of the signal peptide is clearly to facilitate cotranslational import into the endoplasmic reticulum (ER) (32, 37), the mechanism of protein transport between the endomembrane system and the apicoplast has not yet been shown experimentally. Confocal microscopy has shown that the apicoplast is spatially associated with both the mitochondria and the endomembrane system, which may facilitate communication between the organelles (21, 30, 33). Recent studies with *T. gondii* apicoplast outer membrane proteins have shown that large vesicle-like structures may be involved in apicoplast protein import (11, 12). Although the trafficking link between the ER and the apicoplast is currently unresolved, it is assumed that entry into the secretory system is equivalent to crossing the outermost apicoplast membrane.

Also unresolved is how apicoplast proteins are subsequently translocated across the next three membranes with the use of only a transit peptide (29). Initially, translocation across the inner two membranes was hypothesized to involve homologues of the translocon of the outer and inner chloroplast envelopes (TOC and TIC, respectively), since these two membranes are evolutionarily derived from the plastid of a red algal endosymbiont (8). Further, the conserved use of transit peptides as a targeting motif shared by the chloroplast and the apicoplast implies a common translocation mechanism. However, extensive bioinformatics searches of the *P. falciparum* genome, as well as other fully annotated apicomplexan and diatom genomes, have so far failed to identify any orthologues of TOC components, and the identity of this translocon remains mysterious (18). Putative members of an apicoplast TIC complex, Tic22 (unpublished data cited in references 18 and 31) and Tic20 (34), are identifiable though their similarity to plant and algal Tic homologues. In this paper we characterize *P. falciparum* Tic22 (PfTic22) and show that it is associated with apicoplast membranes.

Recently, a novel ER-associated degradation (ERAD) complex, putatively localized to the apicoplast, has been proposed as the translocation complex across the apicoplast periplastid membrane (second membrane inward from the cytosol) (26). Although ERAD complexes are usually associated with retrotranslocation of unfolded or misfolded proteins from the ER, Sommer et al. (26) have identified homologues of several ERAD components with apicoplast-targeting motifs, including two homologues of Der1 (sDer1-1 and sDer1-2), a putative translocation channel component (39). Here, we characterize the localization, expression profile, and solubility of one of these putative apicoplast periplastid membrane translocons, *P. falciparum* symbiont-derived Der1-1 (PfsDer1-1).

MATERIALS AND METHODS

Cloning and parasite transfection. The PfTic22-leader green fluorescent protein (GFP) chimera was constructed by inserting the first 282 bp of the gene encoding PfTic22 (PFE1460w) into the expression vector pHH2 (37). The Multisite Gateway (Invitrogen) cloning system was used to construct vectors expressing hemagglutinin (HA) tagged PfTic22 (PfTic22-HA) and PfsDer1-1 (PfsDer1-1-HA). Briefly, full-length PfTic22 was amplified from 3D7 genomic DNA (gDNA) and cloned into an intermediate cloning vector, pDONR-221, using BP clonase II recombinase (Invitrogen), according to the manufacturer's protocol. The final PfTic22-HA expression vector was constructed using a 5′ chloroquine resistance transporter (CRT) promoter element and three copies of a 3′ HA epitope (HA×3) tag into the modified expression vector pCHD, which contains the WR99210 resistance cassette (27), using LR clonase II recombinase (Invitrogen). The C-terminal 1,065-bp PfsDer1-1 (PF14_0498) was also amplified from 3D7 gDNA but then cloned into the intermediate cloning vector pDONR-P4-P1R using BP clonase II. LR clonase II was then used to construct the final PfsDer1-1 expression vector, utilizing the pCHD vector without a 5′ promoter element but with two epitope tags at the 3′ end of the PfsDer1-1 gene fragment, protein C, and HA×3, separated by a tobacco etch virus protease cleavage site. The protein C epitope was not utilized in these experiments and is not discussed any further here.

The final expression and integration vectors were transfected into the 3D7 parasite strain using standard protocols (27) and selected for with 5 nM WR99210. PfTic22-HA-expressing parasites were recovered after 24 days of continuous drug selection although integration of this expression cassette was not confirmed until after several months of continuous culturing. PfsDer1-1-HA-expressing parasites were recovered after 20 days, and parasites were cultured on and off drug for 6 days (approximately three life cycles), for a total of three on-drug cycles, to allow the episome to be ejected from wild-type parasites lacking the integrated vector (5).

Southern and Western blot hybridization. For both vectors, single-site integration into genomic DNA was confirmed with Southern blot hybridization (4). Briefly, gDNA was isolated with three rounds of phenol-chloroform extraction from saponin-lysed parasites (27) and digested overnight with SpeI and XbaI for PfTic22-HA parasites and with NdeI for PfsDer1-1-HA parasites. The digested DNA was separated on a 1% agarose gel, blotted on nitrocellulose membrane (GE), and probed with radiolabeled probes generated using the PCR amplicons from the initial cloning procedures (above) with [^{32}P]dCTP and the Prime-a-Gene labeling system (Promega), according to the manufacturer's protocol.

Protein expression was detected by Western blot analysis of saponin-lysed parasites using rat anti-HA antibodies (Roche) followed by horseradish peroxidase-conjugated anti-rat (Dako). Parasite cultures were tightly synchronized with two treatments in 5% sorbitol (16) 12 h apart (7) and harvested every 8 h between 4 and 52 h after the second synchronization step.

IFAs. Immunofluorescence assays (IFAs) and confocal microscopy were performed on parasites fixed in 4% paraformaldehyde and 0.015% glutaraldehyde in phosphate-buffered saline (PBS), pH 7.3 (27), using a Leica SP2 confocal microscope. HA was detected with rat anti-HA (Roche) and Alexa Fluor 488-conjugated anti-rat antibodies (Invitrogen). Acyl carrier protein (ACP) was detected with anti-ACP (as described in reference37) and Alexa Fluor 546-conjugated anti-rabbit antibodies (Invitrogen).

Solubilization assays. Parasites expressing either PfTic22-HA or PfsDer1-1-HA were separated from erythrocytes using saponin lysis, and total protein was estimated using the Bradford assay. Saponin pellets containing a total of 1.5 mg of protein were used in each assay and resuspended in 1.5 ml of ice-cold hypotonic buffer (1 mM HEPES-NaOH, pH 7.4, 2 mM EGTA, 2 mM dithiothreitol, and 1× protease inhibitor cocktail [Roche]). The saponin-lysed cell slurry was mechanically lysed on ice using a Dounce homogenizer, consisting of a glass pestle with a Teflon pestle attached to a hand drill. Each saponin slurry was subjected to 10 strokes of 30 s with 30-s intervals. Large insoluble cell debris and unlysed cells were removed with a slow-speed spin (1,500 × *g* for 10 min at 4°C) prior to a high-speed spin (16,100 × *g* for 30 min at 4°C) to separate soluble and insoluble fractions. Equal amounts of the pellet fraction were then resuspended in either 0.2 M Na_2CO_2 or 1% Triton X-100 for 30 min at 4°C. These treatments were then centrifuged (16,100 × *g* for 30 min at 4°C) to separate the supernatant from the pellet. Equal amounts of protein were then analyzed by Western blotting.

Triton X-114 solubilization of cells expressing PfsDer1-1-HA was performed by resuspending saponin-lysed parasites in PBS containing 1% Triton X-114, 2 mM EGTA, and 1× protease inhibitor cocktail for 30 min on ice (20). Insoluble cell debris was removed by a high-speed spin (16,100 × *g* for 10 min at 4°C). The extract was phase partitioned by condensation (for 2 min at 37°C), followed by centrifugation (16,100 × g for 5 min at room temperature) on a sucrose cushion consisting of 6% sucrose and 0.06% Triton X-114 in PBS. The layer above the sucrose cushion in this first round of partitioning was the Triton X-114-soluble fraction while the layer below the sucrose was subjected to a second round of phase partitioning. The layer above the sucrose in this second partitioning was the soluble (wash) fraction while the layer below was the Triton X-114-insoluble fraction.

Antibody generation. Anti-PfTic22 antibodies were generated by immunization of rabbits with a peptide from the mature PfTic22 protein (residues 62 to 283) tagged with an N-terminal poly-His tag in the pET30a expression vector

(Novagen), overexpressed in *Escherichia coli* [strain BL21(DE3)] and purified by affinity chromatography on a Ni^{2+}-agarose column according to the manufacturer's recommendations (Qiagen). Anti-PfsDer1-2 antibodies were raised in rabbits by immunization with the peptide IKDCVSKYTSRSSTNN (Invitrogen) and affinity purified against the peptide using a cyanogen bromide-Sepharose column, according to the manufacturer's protocol (Roche).

RESULTS AND DISCUSSION

PfTic22 is an apicoplast-localized protein. PfTic22 was identified from BlastP searches of the *P. falciparum* genome and shares 21% identity (40% similarity) with the garden pea (*Pisum sativum*) Tic22 orthologue. Similar to other Tic22 homologues (14), PfTic22 has no predicted transmembrane domains. Both apicoplast-targeting predictors (the neural network PATS and the rules-based PlasmoAP algorithm) identify a bipartite leader sequence at the N terminus of PfTic22, suggesting that the protein is localized to the apicoplast (Fig. 1A and Table 1). An alignment of Tic22 sequences demonstrates that PfTic22 contains conserved motifs shared by other Tic22 homologues (see Fig. S1 in the supplemental material) (10), and a search of the protein family (PFAM) database using a hidden Markov model detects a Tic22 motif (PF04278) within PfTic22 with a score of 5.8×10^{-08}.

Initially, we tested the apicoplast localization of PfTic22 by expressing a fusion of the N-terminal bipartite leader of PfTic22 (consisting of the first 94 amino acids) and GFP under the control of the Hsp86 promoter, which drives high expression levels of the reporter (Fig. 1B). This PfTic22-leader–GFP chimera localizes to a punctate organelle in early trophozoites that is consistent with stromal apicoplast localization (Fig. 1B). Furthermore, the pattern of GFP fluorescence throughout the life cycle mimics that of other apicoplast-targeted proteins (data not shown). In contrast, plant Tic22 homologues are known to reside in the intermembrane space between the inner and outer chloroplast envelopes (15, 36), tightly associated with the inner membrane via the inner membrane integral membrane protein Tic20 (14). By analogy, we anticipated that PfTic22 would reside between the two innermost apicoplast membranes (which are believed to be homologues of the two plant chloroplast membranes), perhaps attached to the apicoplast inner membrane protein Tic20. However, peripheral apicoplast localization was not observed for the PfTic22-leader–GFP chimera. We reasoned that the stromal localization of the PfTic22-leader–GFP chimera was probably artificial and might be due to either the high expression levels under the Hsp86 promoter or the large GFP moiety disrupting targeting or, most likely, the lack of mature protein sequence, which is likely necessary for intermembrane space localization.

We therefore transfected parasites with full-length PfTic22 tagged with the smaller HA×3 tandem repeat epitope tag under the control of the weaker CRT promoter element (Fig. 1C). This construct was intended to be an episomal expression vector, but an unanticipated single-site integration event (5) occurred such that the tagged exogenous PfTic22-HA gene replaced the endogenous untagged copy, fortuitously resulting in a tagged gene under the control of its native promoter element (Fig. 1C). This integration event was confirmed by Southern blot analysis (Fig. 1D).

We compared the expression profile of PfTic22-HA with that of the native PfTic22 across the 48-h erythrocytic life cycle using

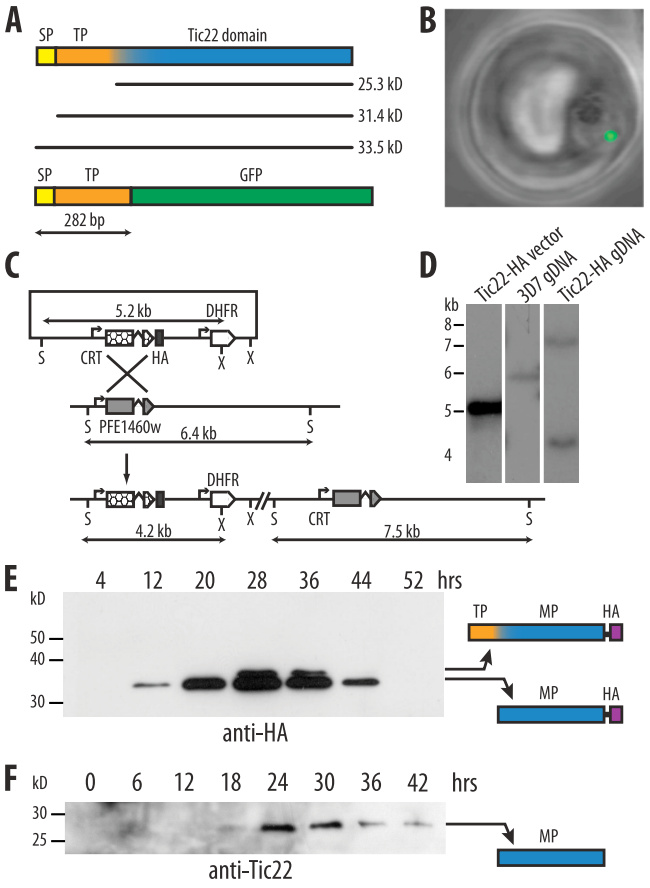

FIG. 1. PfTic22 is a predicted apicoplast protein. (A) PfTic22 has a predicted bipartite leader consisting of a signal peptide (SP; yellow) and transit peptide (TP; orange) and a Tic22 homology domain (blue). The signal peptide cleavage site is robustly predicted (at position 19), whereas the transit peptide cleavage site has not been verified (gradient of orange and blue). Predicted molecular masses were calculated based on primary sequence, with the mature protein region estimated from multiple sequence alignments and PFAM homology. (B) Live fluorescent image of the PfTic22-leader–GFP chimera-carrying parasites showing an apicoplast stromal localization. The construct consists of the first 282 bp of PfTic22 fused to GFP, expressed under the Hsp86 promoter. (C) Construct used to integrate and express PfTic22-HA into gDNA using single-site recombination. The endogenous PfTic22 gene, consisting of two exons and a short intron (light gray boxes separated by a bend) is replaced by the introduced PfTic22 copy (hexagonal patterns) tagged with a C-terminal HA tandem repeat epitope (dark gray box). Although the CRT promoter (labeled square arrow) is present in the construct, the final PfTic22-HA gene is expressed under the endogenous PfTic22 promoter (unlabeled square arrow) due to the integration event. The positions of SpeI (S) and XbaI (X) digest sites used to create the diagnostic fragments for the Southern blot are indicated. (D) Southern blot hybridization using a ^{32}P-labeled PfTic22 probe against purified expression vector, 3D7 (wild type), and PfTic22-HA (transfected) gDNA cut with SpeI and XbaI. (E) Anti-HA Western blotting of PfTic22-HA-expressing parasites harvested at 8-h intervals from 4 to 52 h after two rounds of 5% sorbitol synchronization 12 h apart, where time zero is the time of erythrocyte invasion. The peak of expression is approximately 28 h, showing both the preprocessed (~37 kDa) and mature (~35 kDa) forms of PfTic22. (F) Anti-PfTic22 Western blotting using 3D7 wild-type parasites collected at 6-h intervals from 0 to 42 h after double synchronization showing a peak of expression at 24 h. The observed molecular mass of the mature form of PfTic22-HA is unexpectedly larger than the size predicted from primary sequence analysis. MP, mature protein; DHFR, dihydrofolate reductase.

TABLE 1. Predicted N-terminal leaders of *P. falciparum* Tic22 and Der1 homologues

Protein	Accession no.	Presence of N-terminal leader			
		PlasmoAP output		PATS output	
		Signal peptide[a]	Transit peptide[b]	Decision	Confidence
PfTic22	PFE1460w	4/4	5/5	Yes	0.946
PfsDer1-l	PF14_0498	4/4	5/5	Yes	0.994
PfsDer1-2	PFC0590c	4/4	5/5	Yes	0.998
PfhDer1-1	PF10_0317	3/4	2/5	No	0.028
PfhDer1-2	PF14_0653	3/4	1/5	Yes	0.652

[a] SignalP output showing the probability of a signal peptide being present scored against four parameters, including probability of signal peptide, probability of cleavage site, cleavage site position, and signal peptide length.

[b] The probability of a transit peptide being present scored against five parameters, including the ratio of basic to acidic residues, an enrichment of lysines and asparagines, and the position of basic amino acids.

antibodies against the tag and polyclonal antibodies raised against the recombinantly expressed mature form of PfTic22 (Fig. 1E and F). As expected, PfTic22-HA has an expression profile that is similar to that of the native PfTic22 protein, which is consistent with retention of the native promoter during integration of the tag (Fig. 1C). Both PfTic22-HA and PfTic22 are detectable between 12 and 44 h after invasion, with protein amounts peaking at approximately 24 to 28 h, the early- to mid-trophozoite stage (Fig. 1E and F). Two isoforms of PfTic22-HA are detectable: the higher-molecular-mass species (~37 kDa) likely corresponds to the unprocessed form still bearing its transit peptide, whereas the more abundant lower-molecular-mass species (~35 kDa) most likely corresponds to the mature form of the protein (see Table S1 in the supplemental material). Antibodies to native PfTic22 detect only one protein, which we conclude to be the more abundant mature form of the native protein (Fig. 1E). Although the preprocessed band is approximately the expected size (see Table S1 in the supplemental material), the mature proteins for both the native PfTic22 and PfTic22-HA migrate at a slower rate than predicted, most likely because the actual site of transit peptide cleavage occurs upstream of where the homology of PfTic22 to other orthologues commences. To exclude the possibility of aberrant protein migration, possibly due to incomplete protein unfolding, proteins extracted from a whole-cell lysate were fully denatured in 8 M urea and resolved with 8 M urea–sodium dodecyl sulfate-polyacrylamide gel electrophoresis (see Fig. S2 in the supplemental material). Under these conditions we found that PfTic22-HA migrated only slightly faster than in the absence of urea by approximately 1 kDa, further suggesting that cleavage of the transit peptide occurs upstream of the Tic22 homology.

One consequence of the integration event is the displacement of the endogenous, untagged PfTic22 gene to be driven by the CRT promoter (Fig. 1C). CRT is a relatively weak promoter, and we did not detect expression of the untagged protein in the PfTic22-HA integrant using our antibodies to the native protein (data not shown), suggesting that the native protein is rendered irrelevant.

IFAs of parasites expressing full-length PfTic22-HA confirms the predicted peripheral apicoplast localization (Fig. 2). Close inspection showed that PfTic22-HA expression pattern does not overlap that of the stromal marker, ACP. Rather, PfTic22-HA appears to envelop one side of the stroma, generally in a U-shaped distribution (Fig. 2A, inset, and B). This localization is clearly different from the GFP localization of the PfTic22leader–GFP chimeric protein, which perfectly overlaps the stromal ACP marker (Fig. 2C). There are two possible explanations for the lopsided distribution of PfTic22-HA around the apicoplast periphery: a physiological cause or an artifact. A physiological explanation might be that the apicoplast has discrete functional sides or facets. Previous work has shown that the *P. falciparum* outer membrane triose phosphate transporter (PfoTPT) has a lopsided distribution (20), and another study has shown that the ER is associated with one side of the apicoplast at ring stage (32). Alternatively, lopsided localization of PfTic22-HA might simply be an artifact of the fixation process whereby lateral diffusion of the target protein within the lipid bilayer might be caused by antibody capping-type interactions. This phenomenon is a distinct possibility considering the small amount of glutaraldehyde used in the standard IFA protocol. Whichever the case, peripheral apicoplast localization of PfTic22-HA parallels the location of Tic22 in plant chloroplasts. Our current data cannot determine which membrane the full-length protein is associated with. We observed PfTic22-HA labeling only in mid-trophozoite parasites (despite analyzing parasites from an asynchronous culture), which is consistent with the Western blot analyses (Fig. 1E).

Details of the targeting mechanism of plant Tic22 to the chloroplast intermembrane space are not known. *P. sativum* Tic22 bears a seemingly canonical transit peptide that would ordinarily result in stromal targeting (14), but *P. sativum* Tic22 probably does not enter the stroma, and its transit peptide appears to be removed independently of the stromal processing peptidase (36). Similarly, PfTic22 bears a seemingly canonical stromal targeting leader (Table 1) that appears to be removed (Fig. 1E), but the protein clearly localizes to the apicoplast periphery (Fig. 2). We conclude from this that nonstromal proteins harbor additional targeting information that current bioinformatics predictors, whether for plant chloroplasts or apicoplasts, are unable to distinguish from the majority of stromal proteins. The mechanism of transit peptide processing for PfTic22 (apparently outside of the stroma) remains an intriguing unresolved question, just at it does in plant chloroplast proteins such as Tic22.

PfTic22 is an apicoplast membrane protein. PfTic22 lacks predicted transmembrane domains, but our IFA results show a peripheral apicoplast localization, and plant homologues of Tic22 are chloroplast membrane-associated proteins (14). To test the solubility of PfTic22, we separated soluble and insoluble proteins by mechanical homogenization and subjected the membranes to carbonate and detergent washes (Fig. 3A). After partitioning, more than half of the mitochondrial matrix protein Hsp60, a control soluble protein, was partially solubilized as expected although some protein also remained in the pellet fraction, probably due to incomplete organelle lysis (Fig. 3A, lane 1). In contrast, PfTic22 was found completely within the pellet fraction (Fig. 3A, lane 2), confirming that it is an insoluble membrane protein. Treatment of the membrane protein fraction with alkali (0.2 M Na_2CO_3) indicated that PfTic22-HA is a peripheral membrane protein and not an intrinsic membrane protein since alkali treatment redistributed

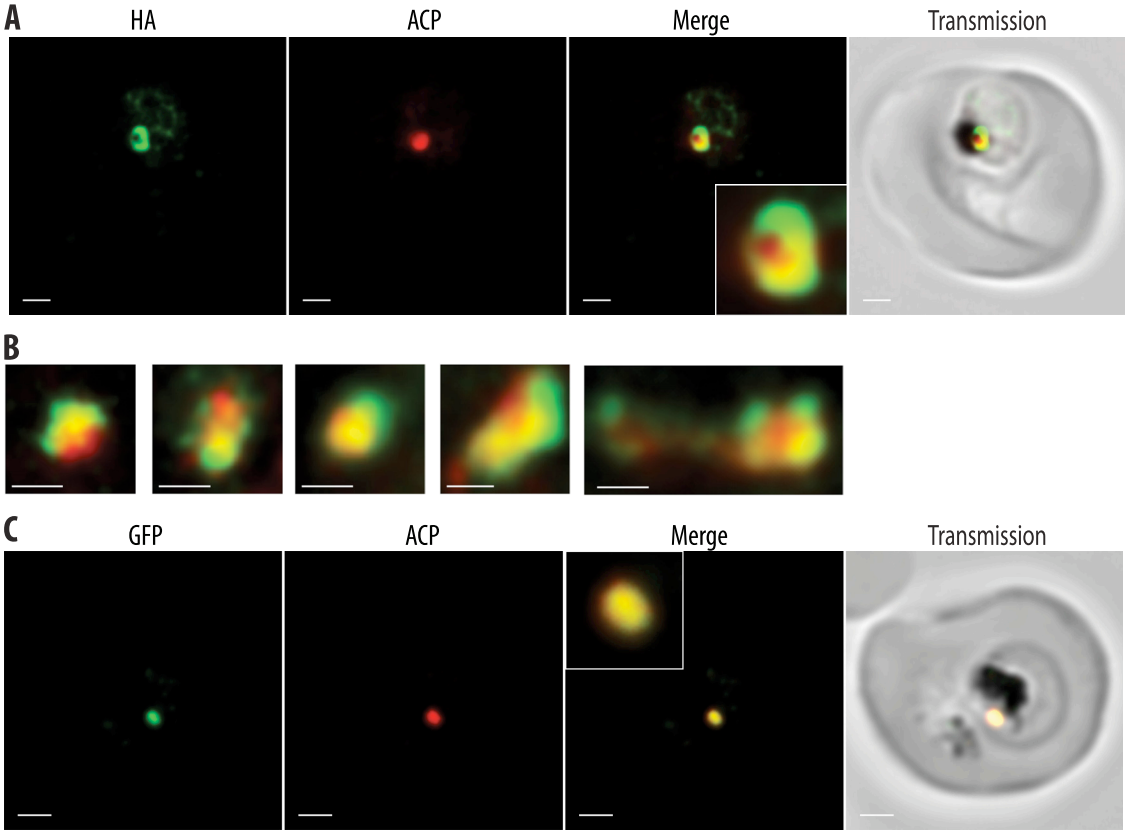

FIG. 2. PfTic22-HA is localized to the periphery of the apicoplast. (A) Confocal image of chemically fixed PfTic22-HA-carrying parasites labeled with anti-HA (green) and anti-ACP antibodies (red), showing that PfTic22-HA is associated with ACP (merge) but is localized to the periphery. Scale bar, 1 μm. The inset shows a zoom of ×3.3. (B) More examples of peripheral localization, similar to the inset above. Scale bar, 0.5 μm. (C) Colocalization of the GFP fluorescence from the PfTic22leader–GFP chimera and with anti-ACP, which does not exhibit a peripheral distribution. Scale bar, 1 μm.

a large component of PfTic22-HA into the soluble phase (Fig. 3A, lane 3). PfTic22-HA was also partially solubilized by Triton X-100 treatment (Fig. 3A, lane 7). PfTic22 is thus largely a peripheral, apicoplast membrane-associated protein.

Overall, PfTic22 shares many similarities to its plant Tic22 orthologues, including its amino acid sequence, solubility, and peripheral plastid localization. As such, we suggest that PfTic22 may also interact with PfTic20 and may have a role in protein import into the plastid, similar to its plant Tic22 counterparts.

***P. falciparum* contains two apicoplast Der1 homologues.** In addition to the TIC complex, we also investigated components of the apicoplast-localized ERAD components as part of our focus on putative apicoplast translocation machinery. Sommer et al. (26) identified several ERAD components bearing plastid localization signals in a diatom and several apicomplexan genomes and postulated that this predicted plastid-localized ERAD complex had been coopted for apicoplast protein import during the conversion of the endosymbiont to a complex plastid (26). We focused particularly on the putative *P. falciparum* homologues of Der1, one of the leading candidates predicted to form the transmembrane channel of the ERAD complex (39). In total, Sommer et al. (26) identified four *P. falciparum* Der1 proteins, two of which have predicted apicoplast leaders: PfsDer1-1 (PF14_0498), and PfsDer1-2 (PFC0590c). The two other homologues are putatively ER-localized proteins, containing only signal peptide N termini: PfhDer1-1 (PF10_0317) and PfhDer1-2 (PF14_0653), where "h" denotes host of the endosymbiont, which, in this instance, is the parasite itself and not the human or mosquito host (26).

Our sequence analysis of these *P. falciparum* sequences concurs with these reported findings. We used a reciprocal BlastP approach to identify 71 Der1 sequences across several apicomplexan genomes, as well as plant, animal, green and red algae, and cyanobacteria (see Table S2 in the supplemental material). A ClustalX alignment of these sequences shows that all four *P. falciparum* proteins contain sequence motifs conserved among other Der1 proteins (see Fig. S3 in the supplemental material). Closer inspection of the alignment shows that PfsDer1-1, along with its apicomplexan orthologues, is more similar to the sDer1-1 sequences from the genomes of the two diatoms *Phaeodactylum tricornutum* (PtsDer1-1) and *Thalassiosira pseudonana* than the sDer1-2 sequences. Conversely, PfsDer1-2 is more similar in sequence to the diatom sDer1-2 sequences. For instance, PfsDer1-1 lacks the conserved proline and tryptophan residues at positions 191 and 466, respectively, a property shared by the diatom sDer1-1 sequences at those positions (see Fig. S3 in the supplemental material). The PfsDer1-2 sequence lacks a conserved glycine at position 512, similar to the diatom sDer1-2 sequences. A phylogeny calculated from

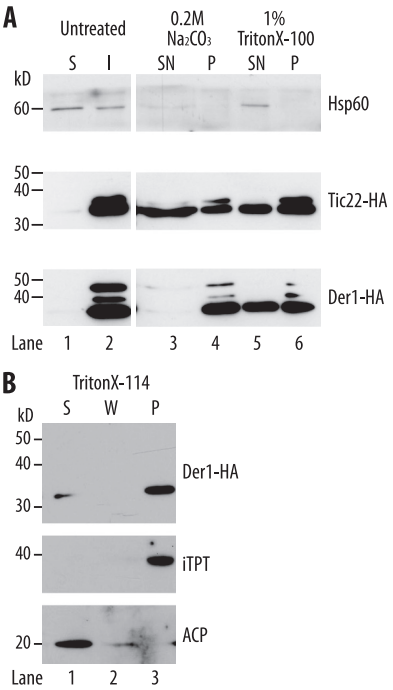

FIG. 3. Both PfTic22-HA and PfsDer1-1-HA are membrane proteins. (A) Saponin-extracted parasites expressing either PfTic22-HA or PfsDer1-1-HA were mechanically lysed with a Dounce homogenizer, and proteins were separated into soluble (S) and insoluble (I) fractions. Equal amounts of the insoluble fractions were then treated with either carbonate (0.2 M Na_2CO_3) or detergent (1% Triton X-100) and then separated into supernatant (SN) and pellet (P) fractions. Both PfTic22-HA and PfsDer1-1-HA were predominantly in the insoluble fraction of the untreated membranes (lane 2) while more than half of Hsp60 (a soluble protein control) was extracted into the soluble phase (lane 1). PfTic22-HA was extracted into the soluble phase by carbonate treatment (lane 3), indicating that it is peripherally membrane associated, whereas PfsDer1-1-HA remained insoluble (lane 4), indicating that it is an integral membrane protein. Both proteins were partially solubilized by Triton X-100 (lane 5) although the majority of the protein remained insoluble (lane 6). (B) Triton X-114 phase partitioning also shows that PfsDer1-1-HA is an integral membrane protein since it remained in the pellet fraction (P), which is the Triton X-114-insoluble phase (lane 3), similar to iTPT, the transmembrane α-helical membrane protein, but different from the stromal marker ACP, which was in the soluble phase (lane 1). Lane 2 contains the wash (W) fraction from the soluble layer of the second-phase partitioning.

this alignment confirms that PfsDer1-1 forms well-supported clades with the diatom sDer1-1 proteins, while PfsDer1-2 forms a distinct clade with the diatom sDer1-2 homologues (data not shown). Together, these observations support the proposed hypothesis that the recruitment of ERAD to the apicoplast most likely occurred prior to the divergence of apicomplexan parasites from the heterokont lineage, which lends support to the chromalveolate hypothesis (26).

We previously suggested that PfsDer1-2 might reside in the second apicoplast membrane (counting out from the inside) and replace the plant chloroplast outer membrane translocon incorporating Toc75, which appears to be absent from apicoplasts (29). However, this hypothesis is not supported by recent data from Hempel et al. (9), who used the split GFP system in *P. tricornutum* to show that both of the two apicoplast-targeted PtsDer1 paralogues most likely localize to the periplastid membrane, with the C terminus situated in the periplastid compartment (9). In addition, the authors showed with coimmunoprecipitation experiments that both of the PtsDer1 paralogues interact both homotypically and heterotypically (9). We infer from these observations that it is likely that PfsDer1-1 and PfsDer1-2 also localize to the periplastid membrane and most probably interact both homotypically and heterotypically.

Based on their N-terminal targeting motifs, it appears that *T. gondii*, *Babesia bovis*, and both *Theileria annulata* and *Theileria parvum* encode only one homologue of sDer1 each (see Fig. S3 in the supplemental material). Given the observation that both *P. tricornutum* and *P. falciparum* contain two sDer1 homologues that interact, it could be that a second, divergent sDer1 homologue not identified by our reciprocal BlastP approach exists in these other apicomplexan genomes. In contrast, all three *Cryptosporidium* sp. genomes lack any sDer1 homologues but still encode two putative hDer1 paralogues (see Fig. S3 in the supplemental material), which is consistent with the total loss of the apicoplast in these apicomplexans.

In this analysis, we used a manually curated gene model for the second predicted apicoplast-localized Der1 homologue (Fig. 4A). The initial gene model encompasses a very large two-exon open reading frame that results in a protein with a predicted molecular mass of 220 kDa, which is markedly larger than other Der1 homologues. Antibodies raised against a peptide from the mature region of PfsDer1-2 detect a 36-kDa protein (Fig. 4B), which is commensurate with our new gene model. The syntenic orthologues of the gene encoding PfsDer1-2 for both *Plasmodium vivax* (PVX_119810) and *Plasmodium knowlesi* (PKH_082580) were modified in a similar way.

Full-length PfsDer1-1 localizes to the apicoplast periphery. Previously, Sommer et al. (26) fused the N-terminal leader of PfsDer1-1 to GFP and showed that this bipartite leader was sufficient to target the reporter to the apicoplast stroma (26), reminiscent of the PfTic22-leader–GFP chimera described above (Fig. 1B). While this result confirmed that PfsDer1-1 is not an ER protein and implicates it in apicoplast protein trafficking, it does not indicate whether PfsDer1-1 is an apicoplast membrane protein. We utilized single-site recombination integration (5) to create parasites expressing full-length PfsDer1-1 with an HA×3 tag under the control of the native PfsDer1-1 promoter (Fig. 4C). The integration vector encoded approximately 1 kb of the C-terminal portion of PfsDer1-1, lacking the first 42 bp of the coding sequence. Since the vector lacks both a promoter region and a translation initiation codon, the recombination event generates a single complete gene copy of PfsDer1-1 tagged with a C-terminal HA×3 epitope. Integration was confirmed by Southern blot analysis (Fig. 4D). Some vector is still detectable in the mixed parasite culture, which may represent parasites that contain multiple insertions of the episomal vector at the gDNA site or parasites containing episomal vectors that had not yet undergone integration. However, as the episome does not encode a complete coding region (Fig. 5C), these vector sequences do not affect our assays.

IFAs showed that PfsDer1-1-HA localizes to the apicoplast, but as with PfTic22, PfsDer1-1-HA encompasses the stromal ACP signal rather than overlapping with it (Fig. 5). Full-length PfsDer1-1-HA is thus a peripheral apicoplast protein. This result differs from previous observations made by Sommer et al. (26), where fusion of the first 416 bp (approximately 138

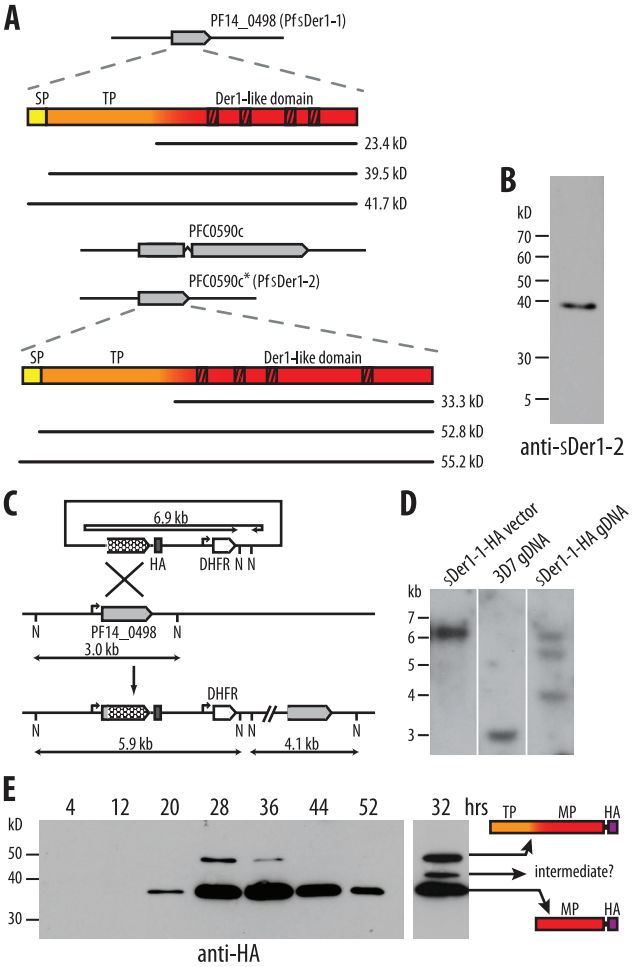

FIG. 4. *P. falciparum* has two predicted apicoplast Der1 homologues. (A) Both PfsDer1-1 and PfsDer1-2 contain predicted apicoplast targeting leaders (yellow and orange), and both contain four predicted transmembrane helices (diagonal boxes) within their Der1 homology domains (red). The mature region is predicted from multiple sequence alignments and PFAM homology. The gene model encoding PfsDer1-2 was modified to exclude the large 3′ exon. (B) Anti-PfsDer1-2 Western blot analysis with antibodies raised against an antigenic peptide (IKDCVSKYTSRSSTNN) indicates a protein with a molecular mass of ~39 kDa, which is more consistent with our new gene model. (C) Single-site recombination integration strategy used to construct PfsDer1-1-HA. Only the 3′ end of the gene is introduced (open-ended box with hexagonal patterns) tagged with HA (dark gray) to replace the endogenous gene (light gray), resulting in a chimeric gene under the control of its endogenous promoter (square arrow). The positions of NdeI (N) restriction sites used to detect integration are indicated. (D) Southern blot hybridization using a ^{32}P-labeled PfsDer1-1 probe against purified expression vector, 3D7 (wild-type), and PfsDer1-1-HA (transfected) gDNA cut with NdeI. (E) Anti-HA Western blotting of PfsDer1-1-HA-expressing parasites harvested at 8-h intervals from 4 to 52 h after two rounds of 5% sorbitol synchronization 12 h apart, where 0 h is the time of erythrocyte invasion. The peak of expression is approximately 28 to 32 h, where the preprocessed (~47 kDa) and mature (36 kDa) forms are detected in addition to a lower-abundance intermediate (41 kDa) form, which may represent a trafficking intermediate. MP, mature protein; DHFR, dihydrofolate reductase; SP, signal peptide; TP, transit peptide.

amino acids) of PfsDer1-1 to GFP expressed episomally under the control of the CRT promoter resulted in apicoplast stromal localization (26). The most likely cause of this difference in localization is that we used the full-length PfsDer1-1, which includes four predicted transmembrane domains. It is also possible that the non-native CRT expression and larger GFP tag may have resulted in mistargeting to the stroma.

Western blot analysis of PfsDer1-1-HA throughout the erythrocytic life cycle of the parasite indicates a broad window of expression throughout the trophozoite and schizont stages, with peak expression around 28 to 32 h after erythrocyte invasion (Fig. 4E). This expression profile largely overlaps with that of the other putative apicoplast import protein PfTic22, which is consistent with a role for PfsDer1-1 in apicoplast protein import. Somewhat unexpectedly, Western blots of PfsDer1-1-HA detect three HA-positive proteins (Fig. 4E). The smallest protein (~36 kDa) is most abundant and most likely corresponds to the processed mature protein although it is larger than expected from in silico predictions (see Table S1 in the supplemental material). The largest species (~47 kDa) most likely corresponds to the preprocessed, transit peptide-bearing form. The third and intermediate species (~41 kDa) is the least abundant and is a possible targeting intermediate en route to its final destination in the periplastid membrane. This intermediate species was unexpected, as most apicoplast proteins have only the preprocessed and mature forms. We note that multiple processing intermediates have also been reported for the *P. falciparum* apicoplast inner membrane TPT protein, PfiTPT (20), and the *T. gondii* peripheral apicoplast membrane protein FtsH1 (12, 13), but the sequence of events and what proteases are involved in processing are not known for any apicoplast membrane proteins. By contrast, no third, intermediate protein species was detected for the apicoplast membrane protein PfTic22 (Fig. 1E).

PfsDer1-1 is an integral apicoplast membrane protein. To confirm membrane localization for PfsDer1-1, we performed detergent solubility tests (Fig. 3). All three mass forms of PfsDer1-1 were pelleted with the insoluble membrane fraction of isolated membranes (Fig. 3, lane 2), consistent with the prediction of four hydrophobic α-helices (Fig. 4A). Alkali treatment (0.2 M Na_2CO_3) did not redistribute PfsDer1-1 into the soluble phase (Fig. 3A, lane 4), indicating that it is not peripherally associated with the membrane. Triton X-100 treatment partially solubilized PfsDer1-1 (lane 7). We also tested the solubility of PfsDer1-1-HA with Triton-X 114 (Fig. 3B), which solubilizes proteins lacking α-helical transmembrane domains (1). PfsDer1-1 remained in the Triton X-114-insoluble fraction, confirming that it contains integral α-helical transmembrane domains (Fig. 3B, lane 3). Triton X-114 treatment solubilized the ACP stromal control (Fig. 3B, lane 1), but PfiTPT, a membrane protein with 10 predicted transmembrane domains (20), remained in the Triton X-114-insoluble fraction (Fig. 3B, lane 3). Together, these results indicate that PfsDer1-1 is an integral membrane protein.

Concluding remarks. We have shown that both PfTic22 and PfsDer1-1 are membrane proteins localized to the periphery of the apicoplast and that both proteins are maximally expressed during the trophozoite stages of the asexual cycle. All these characteristics are consistent with their proposed roles in apicoplast protein translocation, but our results cannot exclude the possibility that both PfTic22 and PfsDer1-1 have functions outside of protein translocation.

An unresolved question is how proteins with seemingly typical bipartite leaders localize to non-stromal locations. With

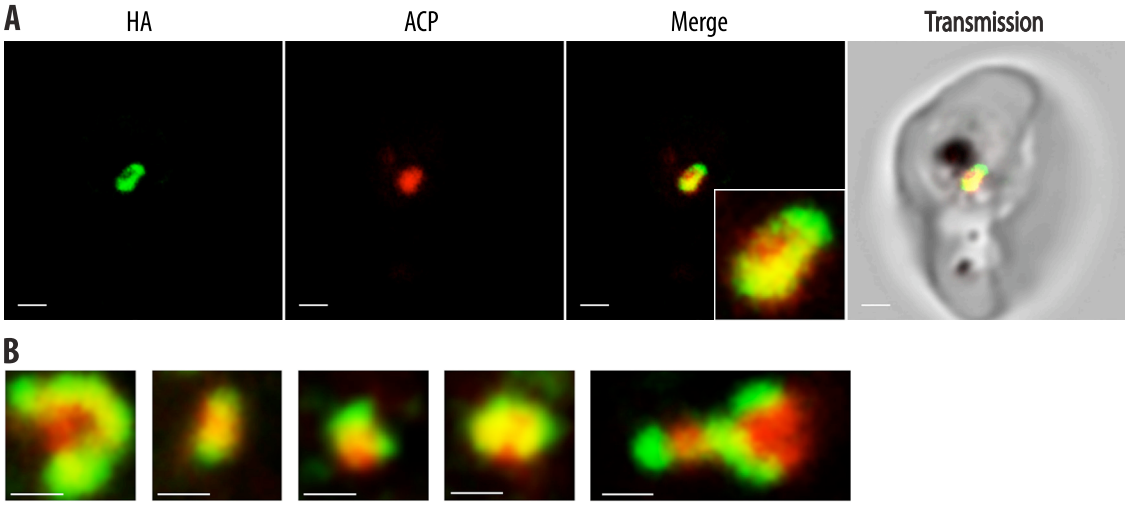

FIG. 5. PfsDer1-1-HA is located at the periphery of the apicoplast. (A) Confocal images of chemically fixed PfsDer1-1-HA parasites labeled with anti-HA (green) and anti-ACP (red) antibodies showing that PfsDer1-1-HA is associated with ACP (merge) but is peripheral, similar to PfTic22-HA. Inset shows a ×3.3 zoom of the localizations. (B) More examples of peripheral localization, similar to the inset above. Scale bar, 0.5 μm.

four bounding membranes, the apicoplast has at least three distinct soluble compartments, and these likely have distinct proteomes. Our results indicate that our initial assumption that all bipartite leader-bearing proteins localize to the stroma needs rethinking. In particular, both PfTic22 and PfsDer1-1 demonstrate that the detection of transit peptide processing (by Western blotting) is not necessarily always an appropriate diagnostic for apicoplast stromal localization.

Although our localization of these candidates in the appropriate location in the malaria parasite plastid lends further weight to their postulated roles in transport and fleshes out earlier genome mining models based solely on sequence similarity (18), the challenge remains to elucidate their precise roles in apicoplast protein translocation and to identify the interacting partners involved in the transport machinery.

ACKNOWLEDGMENTS

We thank E. Handman for kindly help generating anti-PfTic22 antibodies and for advice on the manuscript. We thank S. Gould, D. Morse, G. van Dooren, and R. Waller for constructive discussions.

M.K. was supported by an Australian Postgraduate Award, and C.J.T. was supported by a Melbourne Research Scholarship. G.I.M. is an Australian Research Council Federation Fellow and a Howard Hughes International Research Scholar. Program Grant support from the National Health and Medical Research Council is gratefully acknowledged.

The Australian Red Cross generously supplied human red blood cells.

REFERENCES

1. **Bordier, C.** 1981. Phase separation of integral membrane proteins in Triton X-114 solution. J. Biol. Chem. **256:**1604–1607.
2. **Cavalier-Smith, T.** 2003. Genomic reduction and evolution of novel genetic membranes and protein-targeting machinery in eukaryote-eukaryote chimaeras (meta-algae). Philos. Trans. R. Soc. Lond. B **358:**109–134.
3. **Chaubey, S., A. Kumar, D. Singh, and S. Habib.** 2005. The apicoplast of *Plasmodium falciparum* is translationally active. Mol. Microbiol. **56:**81–89.
4. **Crabb, B. S., B. M. Cooke, J. C. Reeder, R. F. Waller, S. R. Caruana, K. M. Davern, M. E. Wickham, G. V. Brown, R. L. Coppel, and A. F. Cowman.** 1997. Targeted gene disruption shows that knobs enable malaria-infected red cells to cytoadhere under physiological shear stress. Cell **89:**287–296.
5. **Crabb, B. S., M. Rug, T. W. Gilberger, J. K. Thompson, T. Triglia, A. G. Maier, and A. F. Cowman.** 2004. Transfection of the human malaria parasite *Plasmodium falciparum*. Methods Mol. Biol. **270:**263–276.
6. **Foth, B. J., S. A. Ralph, C. J. Tonkin, N. S. Struck, M. Fraunholz, D. S. Roos, A. F. Cowman, and G. I. McFadden.** 2003. Dissecting apicoplast targeting in the malaria parasite *Plasmodium falciparum*. Science **299:**705–708.
7. **Goodman, C. D., V. Su, and G. I. McFadden.** 2007. The effects of antibacterials on the malaria parasite *Plasmodium falciparum*. Mol. Biochem. Parasitol. **152:**181–191.
8. **Gould, S. B., R. F. Waller, and G. I. McFadden.** 2008. Plastid evolution. Annu. Rev. Plant Biol. **59:**491–517.
9. **Hempel, F., L. Bullmann, J. Lau, S. Zauner, and U. G. Maier.** 17 April 2009, posting date. ERAD-derived pre-protein transport across the 2nd outermost plastid membrane of diatoms. Mol. Biol. Evol. doi:10.1093/molbev/msp079.
10. **Kalanon, M., and G. I. McFadden.** 2008. The chloroplast protein translocation complexes of *Chlamydomonas reinhardtii*: a bioinformatic comparison of Toc and Tic components in plants, green algae and red algae. Genetics **179:**95–112.
11. **Karnataki, A., A. Derocher, I. Coppens, C. Nash, J. E. Feagin, and M. Parsons.** 2007. Cell cycle-regulated vesicular trafficking of *Toxoplasma* APT1, a protein localized to multiple apicoplast membranes. Mol. Microbiol. **63:**1653–1668.
12. **Karnataki, A., A. E. Derocher, I. Coppens, J. E. Feagin, and M. Parsons.** 2007. A membrane protease is targeted to the relict plastid of *Toxoplasma* via an internal signal sequence. Traffic **8:**1543–1553.
13. **Karnataki, A., A. E. DeRocher, J. E. Feagin, and M. Parsons.** 2009. Sequential processing of the *Toxoplasma* apicoplast membrane protein FtsH1 in topologically distinct domains during intracellular trafficking. Mol. Biochem. Parasitol. **166:**126–133.
14. **Kouranov, A., X. Chen, B. Fuks, and D. J. Schnell.** 1998. Tic20 and Tic22 are new components of the protein import apparatus at the chloroplast inner envelope membrane. J. Cell Biol. **143:**991–1002.
15. **Kouranov, A., H. Wang, and D. J. Schnell.** 1999. Tic22 is targeted to the intermembrane space of chloroplasts by a novel pathway. J. Biol. Chem. **274:**25181–25186.
16. **Lambros, C., and J. P. Vanderberg.** 1979. Synchronization of *Plasmodium falciparum* erythrocytic stages in culture. J. Parasitol. **65:**418–420.
17. **Martin, W., and R. G. Herrmann.** 1998. Gene transfer from organelles to the nucleus: how much, what happens, and why? Plant Physiol. **118:**9–17.
18. **McFadden, G. I., and G. G. van Dooren.** 2004. Evolution: red algal genome affirms a common origin of all plastids. Curr. Biol. **14:**R514–R516.
19. **Moore, R., M. Oborník, J. Janouskovec, T. Chrudimský, M. Vancová, D. Green, S. Wright, N. Davies, C. J. Bolch, K. Heimann, J. Slapeta, O. Hoegh-Guldberg, J. Logsdon, and D. Carter.** 2008. A photosynthetic alveolate closely related to apicomplexan parasites. Nature **451:**959–963.
20. **Mullin, K. A., L. Lim, S. A. Ralph, T. P. Spurck, E. Handman, and G. I. McFadden.** 2006. Membrane transporters in the relict plastid of malaria parasites. Proc. Natl. Acad. Sci. USA **103:**9572–9577.
21. **Okamoto, N., T. P. Spurck, C. D. Goodman, and G. I. McFadden.** 2009. Apicoplast and mitochondrion in gametocytogenesis of *Plasmodium falciparum*. Eukaryot. Cell. **8:**128–132.

22. **Ralph, S.** 2004. Evolutionary pressures on apicoplast transit peptides. Mol. Biol. Evol. **21:**2183–2194.
23. **Ralph, S. A., G. G. van Dooren, R. F. Waller, M. J. Crawford, M. J. Fraunholz, B. J. Foth, C. J. Tonkin, D. S. Roos, and G. I. McFadden.** 2004. Metabolic maps and functions of the *Plasmodium falciparum* apicoplast. Nat. Rev. Microbiol. **2:**203–216.
24. **Rowe, A. K.** 2006. Analysis of deaths with an unknown cause in epidemiologic analyses of mortality burden. Trop. Med. Int. Health. **11:**540–550.
25. **Seow, F., S. Sato, C. Janssen, M. Riehle, A. Mukhopadhyay, R. Phillips, R. Wilson, and M. Barrett.** 2005. The plastidic DNA replication enzyme complex of. Mol. Biochem. Parasitol. **141:**145–153.
26. **Sommer, M. S., S. B. Gould, P. Lehmann, A. Gruber, J. M. Przyborski, and U. G. Maier.** 2007. Der1-mediated preprotein import into the periplastid compartment of chromalveolates? Mol. Biol. Evol. **24:**918–928.
27. **Tonkin, C.** 2004. Localization of organellar proteins in *Plasmodium falciparum* using a novel set of transfection vectors and a new immunofluorescence fixation method. Mol. Biochem. Parasitol. **137:**13–21.
28. **Tonkin, C. J., B. J. Foth, S. A. Ralph, N. Struck, A. F. Cowman, and G. I. McFadden.** 2008. Evolution of malaria parasite plastid targeting sequences. Proc. Natl. Acad. Sci. USA **105:**4781–4785.
29. **Tonkin, C. J., M. Kalanon, and G. I. McFadden.** 2008. Protein targeting to the malaria parasite plastid. Traffic **9:**166–175.
30. **Tonkin, C. J., J. A. Pearce, G. I. McFadden, and A. F. Cowman.** 2006. Protein targeting to destinations of the secretory pathway in the malaria parasite *Plasmodium falciparum*. Curr. Opin. Microbiol. **9:**381–387.
31. **Tonkin, C. J., D. S. Roos, and G. I. McFadden.** 2006. N-terminal positively charged amino acids, but not their exact position, are important for apicoplast transit peptide fidelity in *Toxoplasma gondii*. Mol. Biochem. Parasitol. **150:**192–200.
32. **Tonkin, C. J., N. S. Struck, K. A. Mullin, L. M. Stimmler, and G. I. McFadden.** 2006. Evidence for Golgi-independent transport from the early secretory pathway to the plastid in malaria parasites. Mol. Microbiol. **61:**614–630.
33. **van Dooren, G. G., M. Marti, C. J. Tonkin, L. M. Stimmler, A. F. Cowman, and G. I. McFadden.** 2005. Development of the endoplasmic reticulum, mitochondrion and apicoplast during the asexual life cycle of *Plasmodium falciparum*. Mol. Microbiol. **57:**405–419.
34. **van Dooren, G. G., C. Tomova, S. Agrawal, B. M. Humbel, and B. Striepen.** 2008. *Toxoplasma gondii* Tic20 is essential for apicoplast protein import. Proc. Natl. Acad. Sci. USA **105:**13574–13579.
35. **Vaughan, A., M. T. O'Neill, A. S. Tarun, N. Camargo, T. Phuong, A. Aly, A. F. Cowman, and S. Kappe.** 2009. Type II fatty acid synthesis is essential only for malaria parasite late liver stage development. Cell Microbiol. **11:**506–520.
36. **Vojta, L., J. Soll, and B. Bölter.** 2007. Protein transport in chloroplasts—targeting to the intermembrane space. FEBS J. **274:**5043–5054.
37. **Waller, R. F., M. B. Reed, A. F. Cowman, and G. I. McFadden.** 2000. Protein trafficking to the plastid of *Plasmodium falciparum* is via the secretory pathway. EMBO J. **19:**1794–1802.
38. **Wilson, R. J., P. W. Denny, P. R. Preiser, K. Rangachari, K. Roberts, A. Roy, A. Whyte, M. Strath, D. J. Moore, P. W. Moore, and D. H. Williamson.** 1996. Complete gene map of the plastid-like DNA of the malaria parasite *Plasmodium falciparum*. J. Mol. Biol. **261:**155–172.
39. **Ye, Y., Y. Shibata, C. Yun, D. Ron, and T. A. Rapoport.** 2004. A membrane protein complex mediates retro-translocation from the ER lumen into the cytosol. Nature **429:**841–847.
40. **Yu, M., T. R. Kumar, L. J. Nkrumah, A. Coppi, S. Retzlaff, C. D. Li, B. J. Kelly, P. A. Moura, V. Lakshmanan, J. S. Freundlich, J. C. Valderramos, C. Vilcheze, M. Siedner, J. H. Tsai, B. Falkard, A. B. Sidhu, L. A. Purcell, P. Gratraud, L. Kremer, A. P. Waters, G. Schiehser, D. P. Jacobus, C. J. Janse, A. Ager, W. R. Jacobs, J. C. Sacchettini, V. Heussler, P. Sinnis, and D. A. Fidock.** 2008. The fatty acid biosynthesis enzyme FabI plays a key role in the development of liver-stage malarial parasites. Cell Host Microbe **4:**567–578.
41. **Zhu, G., M. J. Marchewka, and J. S. Keithly.** 2000. *Cryptosporidium parvum* appears to lack a plastid genome. Microbiology **146:**315–321.
42. **Zuegge, J., S. Ralph, M. Schmuker, G. I. McFadden, and G. Schneider.** 2001. Deciphering apicoplast targeting signals: feature extraction from nuclear-encoded precursors of *Plasmodium falciparum* apicoplast proteins. Gene **280:**19–26.